



Proceeding Paper

# Early Detection of Volatile Tumor Biomarkers Using Chemoresistive Sensors and MEMS-Based Preconcentration: A Study on K562 Cell Line ‡

Melissa Tamisari 1,\*,†, Elena Spagnoli 2,†, Maria Teresa Altieri 3, Michele Astolfi 1, Monica Borgatti 3, Giulia Breveglieri 3, Ivan Elmi 2, Vincenzo Guidi 4, Luca Masini 2, Arianna Rossi 4, Giuseppe Sabbioni 3, Emanuela Tavaglione 4, Stefano Zampolli 2 and Barbara Fabbri 4

- Department of Neuroscience and Rehabilitation, University of Ferrara, Via Borsari 46, 44121 Ferrara, Italy; michele.astolfi@unife.it
- National Research Council (CNR), Institute for Nanostructured Materials (ISMN), Via P. Gobetti 101, 40129 Bologna, Italy; elenaspagnoli@cnr.it (E.S.); ivan.elmi@cnr.it (I.E.); luca.masini@cnr.it (L.M.); stefano.zampolli@cnr.it (S.Z.)
- <sup>3</sup> Department of Life Sciences and Biotechnology, University of Ferrara, Via Borsari 46, 44121 Ferrara, Italy; mariateresa.altieri@unife.it (M.T.A.) monica.borgatti@unife.it (M.B.); giulia.breveglieri@unife.it (G.B.); giuseppe.sabbioni@unife.it (G.S.)
- <sup>4</sup> Department of Physics and Earth Science, University of Ferrara, Via Saragat 1/C, 44122 Ferrara, Italy; vincenzo.guidi@unife.it (V.G.); arianna.rossi@unife.it (A.R.); emanuela.tavaglione@unife.it (E.T.); barbara.fabbri@unife.it (B.F.)
- \* Correspondence: melissa.tamisari@unife.it
- <sup>+</sup> M.T. and E.S. contributed equally to this work.
- <sup>‡</sup> Presented at the 12th International Electronic Conference on Sensors and Applications (ECSA-12), 12–14 November 2025; Available online: https://sciforum.net/event/ECSA-12.

## Abstract

The analysis of volatile organic compounds emitted by cell cultures provides a non-invasive method for monitoring metabolic and oxidative stress states. However, detection is challenged by low volatile organic compounds concentrations and high sample humidity. This study introduces an integrated system combining a MEMS-based pre-concentrator with an array of n-type metal-oxides chemiresistive gas sensors to analyze emissions from the K562 leukemia cell line. The main goal is to distinguish cellular volatile organic compounds signals from those of the culture medium. To achieve this, the pre-concentrator is used with different temperature-programmed desorption protocols to enhance signal intensity and improve discrimination performance.

**Keywords:** VOCs; chemoresistive gas sensor; low gas emission analysis; preconcentration; cell cultures

Academic Editor(s): Name

Published: date

Citation: Tamisari, M.; Spagnoli, E.; Altieri, M.T.; Astolfi, M.; Borgatti, M.; Breveglieri, G.; Elmi, I.; Guidi, V.; Masini, L.; Rossi, A.; et al. Early Detection of Volatile Tumor Biomarkers Using Chemoresistive Sensors and MEMS-Based Preconcentration: A Study on K562 Cell Line. *Eng. Proc.* 2025, volume number, x.

https://doi.org/10.3390/xxxxx

Copyright: © 2025 by the authors. Submitted for possible open access publication under the terms and conditions of the Creative Commons Attribution (CC BY) license (https://creativecommons.org/license s/by/4.0/).

## 1. Introduction

In recent years, biomedical research has shown a growing interest in identifying non-invasive biomarkers for the early diagnosis of neoplasms, including those of hematological origin such as leukemia. Among the emerging strategies, the analysis of Volatile Organic Compounds (VOCs), which are produced by cellular metabolism, has proven to be particularly promising. VOCs are small gaseous molecules released by cells in response to specific biochemical, metabolic processes, and oxidative stress, and they can directly reflect the pathophysiological state of a cell population.

Eng. Proc. 2025, x, x https://doi.org/10.3390/xxxxx

A fundamental element underlying this approach is the difference between the metabolism of healthy cells and that of cancer cells, i.e., leukemic cells. Healthy cells primarily derive energy through aerobic cellular respiration, an efficient mitochondrial process that leads to the production of carbon dioxide and water with minimal volatile byproducts. Leukemic cells, on the other hand, like many other cancer cells, exhibit an altered metabolic profile characterized by increased anaerobic glycolysis even in the presence of oxygen (the Warburg effect [1]). This phenomenon results in a higher production of metabolic byproducts, including various VOCs such as aldehydes, ketones, alcohols, and hydrocarbons. The collection of these compounds constitutes a metabolic fingerprint that is potentially useful for diagnostic purposes.

For the detection of these VOCs, one of the most promising technologies is represented by chemoresistive devices. Printable chemoresistive gas sensors are particularly advantageous due to their high sensitivity and simple transducer/receptor design, enabling easy production, low costs and miniaturization. Indeed, the principles of gas detection are based on the interaction of gaseous molecules with a nanostructured semiconducting sensing layer, usually made of Metal-Oxides (MOXs), which results in a detectable change in its electrical properties [2,3]. Already widely used in the environmental and agri-food sectors [4,5], chemoresistive gas sensors are also finding applications in the medical field, particularly in the development of tools for cellular metabolic monitoring and early diseases diagnosis or screening [6,7]. However, it is important to select suitable sensing layers for this kind of analysis. Indeed, the sensors must exhibit high selectivity toward VOCs emitted by the cells, while maintaining minimal sensitivity to gaseous interferents originating from the culture medium in which the cells are grown. In particular, the cell culture medium is water-based, and consequently the relative humidity (RH%) of the gaseous sample is high, in the range of 50%. As widely reported in the literature, moisture is highly reactive and can directly interact with the functional material surface, altering the active sites and affecting the electrical properties of the sensor. This interaction may also hinder the detection of gaseous analytes by limiting their adsorption and subsequent reaction [8–12].

Therefore, to detect VOCs from cellular emissions, often present at very low concentrations within a complex mixture of interfering gases, it can be advantageous to subject the gaseous sample to a pre-treatment step. To this end, even restricting the sensors low detection limit, this study proposes the use of a chemoresistive sensor array coupled with a MEMS (Micro-Electro-Mechanical Systems) pre-concentrator [13,14]. This device allows for the capture and accumulation of VOCs molecules from a large volume of air over a defined period, which are then released in a single, concentrated pulse. This process would significantly amplify the signal, enabling the MOXs sensors to detect even faint traces of VOCs that would otherwise remain undetectable.

### 2. Materials and Methods

The overall set-up for detection of gaseous emissions from cells is depicted in Figure 1. This section will describe the biological samples characteristics, sensor development and characterization set-up, the preconcentration system, and finally the experimental workflow.

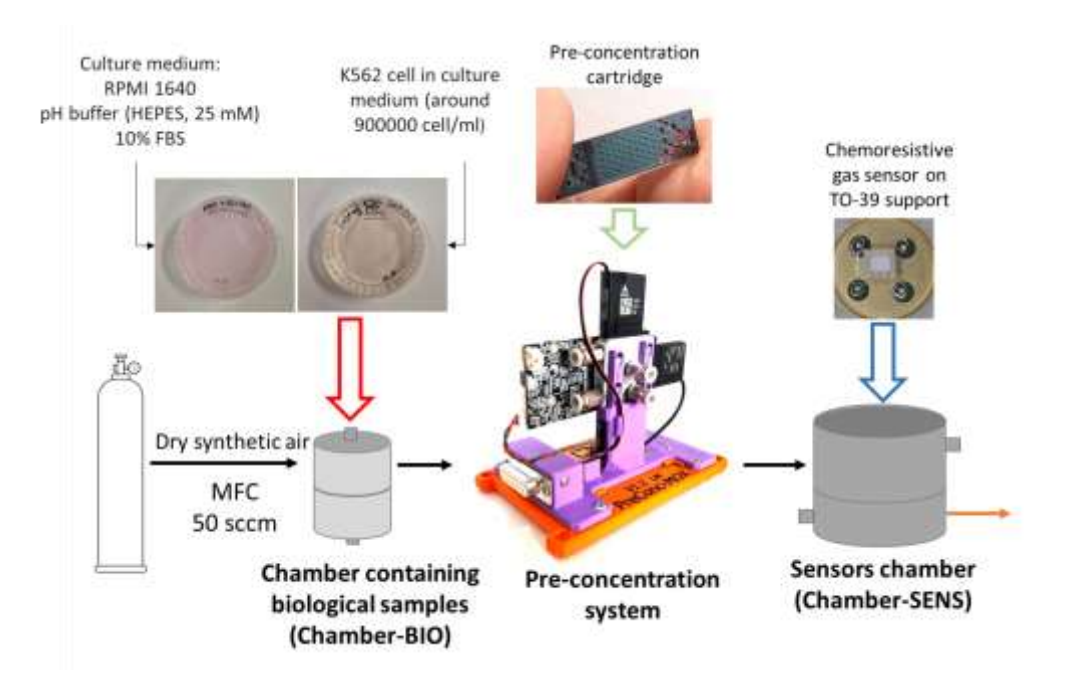


Figure 1. Experimental setup for sensing volatile compounds from cell culture exhalation.

Biological samples. The K562 human leukemia cell line, derived from a patient with chronic myeloid leukemia, was used as the biological case of study. This cell line is a wellestablished standard for investigating hematological neoplasms [15,16]. Cells were cultured in a humidified atmosphere of 5% CO<sub>2</sub>/air at 37 °C in cell culture flasks using RPMI 1640 medium (Carlo Erba, Milan, Italy) supplemented with 10% Fetal Bovine Serum (FBS). The biological samples used for the detection of gaseous emissions consisted of 5 mL of culture medium, with or without K562 cells, placed in a 5 cm diameter Petri dish and buffered with HEPES 25 mM to maintain a physiological pH of 7.0. The cell density was maintained within the range from 0.7 to 0.9 million cells/mL to ensure consistent and comparable measurements of volatile emissions. For gas sensing measurements, the Petri dish containing either only culture medium (BLANK) or the culture medium with K562 cells (K562) was placed on a metallic support inside a hermetically sealed stainless steel chamber (Chamber-BIO), equipped with two gas-tight pneumatic fittings welded to the base and lid. To monitor the health and physiological state of the cell population throughout the experiments, cell viability was quantified using the Muse<sup>TM</sup> Annexin V & Dead Cell Assay (Luminex Corporation, Austin, Texas, USA), following the manufacturer's instructions. This fluorescence-based method allows for the discrimination between live, early apoptotic, late apoptotic, and dead cells by detecting the translocation of phosphatidylserine to the outer cell membrane, a key marker of apoptosis.

Sensor development. The chemoresistive gas sensors employed in this study were fabricated starting from nanostructured MOXs powders based on Au decorated tin dioxide (Au@SnO2), tungsten trioxide (WO3) and a trimetallic solution of tin, titanium and niobium oxides ((Sn,Ti,Nb)xO2). The material synthesis and characterization were detailed in previous works [17,18]. The synthesized powders were subsequently mixed with organic excipients to form homogeneous pastes, and thus screen-printed onto  $2.5 \times 2.5 \text{ mm}^2$  alumina substrates as mesoporous nanostructured thick films (20–30 µm). Each substrate was equipped with interdigitated gold electrodes on the front side for measuring the conductance of the sensing layer and an integrated platinum heater on the rear for its thermal activation to the optimal operating temperature. After sintering at 650 °C for 2 h to ensure mechanical stability, the devices were bonded to a standard TO-39 support using goldwire (diameter 60 µm) thermocompression [17]. Other sensors based on different

materials, like ZnO grains, (W,Sn)xO2 and Pd@SnO2, were considered, but they showed poor preliminary performance in terms of low response level to the biological sample emissions and high influence of humidity on their electrical behaviour.

Sensors electrical characterization set-up. Au@SnO2, WO3 and (Sn,Ti,Nb)xO2-based devices were placed in a customized apparatus (Chamber-SENS), composed of a stainless steel gas test chamber (empty volume 200 cm³) and a sensor data acquisition system. Au@SnO2, WO3, and (Sn,Ti,Nb)xO2 sensor working temperature was setted to 350 °C, 250 °C, and 450 °C, respectively. Indeed, the semiconducting functional layer typically requires thermal activation to promote gas–surface reactions, thereby enhancing sensor response. Additionally, heating facilitates gas desorption, contributing to the reversibility of the detection process and reducing the recovery time. This parameter optimization has been addressed in Rossi et al. [19]. A constant bias voltage of 5 V was applied to the sensor, and its conductance (Gs) was measured using a custom circuit [20] based on an operational amplifier according to the equation:

$$G_s = \frac{V_{out}}{R_f \cdot V_{in}} \tag{1}$$

where  $R_f$  is a known load resistance. The optimal operating temperature for each sensor was determined based on previous work from our sensor laboratory. The sensor response (R) was defined as:

$$R = \frac{G_{gas} - G_{air}}{G_{air}} \tag{2}$$

for reducing gases, where  $G_{gas}$  and  $G_{air}$  are the steady-state conductance values in the target gas and in clean air [21].

Along with the chemoresistive gas sensors, the Chamber-SENS housed a commercially available LM35 temperature sensor and Honeywell HIH-4000 humidity sensor to monitor the stream temperature and RH%.

Preconcentration system. The pre-concentration system was based on a micromachined silicon cartridge containing a sorbent material capable of preferentially retaining the VOCs of interest while allowing most interfering molecules, such as humidity, to pass through. The chip dimension was 25 × 14 × 1.5 mm³. It was realized by bulk micromachining of a 4 in. silicon wafer with a deep reactive ion etching (DRIE) process, followed by an anodic bonding to a Pyrex wafer for encapsulation [13]. A platinum heater, together with a platinum thermistor, were positioned on the back-side of the silicon wafer for precise temperature control. Following encapsulation and dicing, the cartridge was filled with Carbosieve S-III 1000m²/g (sigma-aldrich). The overall set-up is schematically represented in Figure 1 and included also the pre-concentration system hardware and software. It allowed to (i) stabilize the sensors baseline in dry air, (ii) preconcentrate biological sample emissions, (iii) desorb trapped gases in inverse and direct flux, and (iv) set temperature desorption program.

Experiment flow. A certified synthetic air (20% O<sub>2</sub>, 80% N<sub>2</sub>) cylinder was used to provide the carrier flow, transporting the gas emitted from the biological sample inside the Chamber-BIO to the pre-concentrator system, and finally to the Chamber-SENS. The configuration also allowed the gas flow to go directly into the Chamber-SENS if the operator wanted to avoid passing through the pre-concentrator cartridge. This option was used to evaluate the sensors response to water vapor and to the biological samples emissions without the gaseous sample pre-treatment step. Humidified air at controlled RH% was obtained by injecting a fraction of the total synthetic air flux into a gas bubbler filled with deionized water. The final RH% values were cross verified using a commercial humidity

sensor. In all experiments, mass-flow controllers (Brooks) were used to maintain a total flow of 50 sccm.

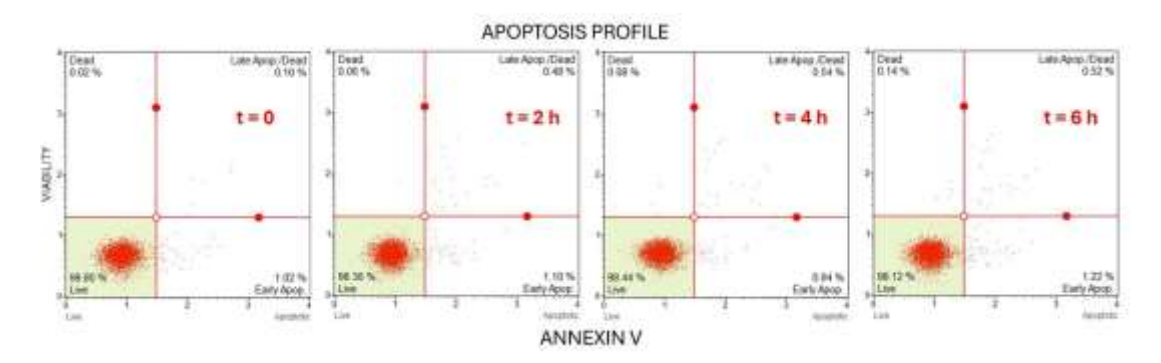
The experimental procedure including the pre-concentrator consisted of several phases. Moreover, two different measurement cycles, Cycle1 and Cycle2, were used.

Cycle1. Firstly, the pre-concentrator was heated to 150 °C for 5 min under a flow of dry air (50 sccm), in order to desorb any residual compounds previously accumulated (Phase 1). In Phase 2, the carrier was conveyed through the Chamber-BIO and then through the pre-concentrator, to collect the emitted gas from the biological sample. After 15 min of accumulation phase, the connections with the Chamber-BIO and the pre-concentrator were closed, directing the air flow directly to the Chamber-SENS, allowing the sensor to return to baseline conditions (Phase 3). During the desorption stage (Phase 4), fluidic access to the pre-concentrator was re-established, while the Chamber-BIO remained isolated. The pre-concentrator was heated to 50 °C, and a reversed flow of dry air (opposite to Phase 2) was applied for 30 min to initiate the desorption process. In Phase 5, the temperature of the pre-concentrator was increased to 150 °C for an additional 30 min to ensure the complete release of the adsorbed compounds. Throughout all Phases, the airflow remained connected to the Chamber-SENS to monitor RH%, identify potential fluidic failures, and detect any gases not retained by the sorbent during the accumulation step.

*Cycle*2. Phase 1 and Phase 2 of Cycle2 were equal to Phase 2 and Phase 3 of Cycle1. The main difference between the two cycles lay in the desorption procedure. Indeed, this time the pre-concentrator was heated from 30 °C to 150 °C over a period of 40 min, followed by a 10-min isothermal hold at 150 °C.

#### 3. Results and Discussion

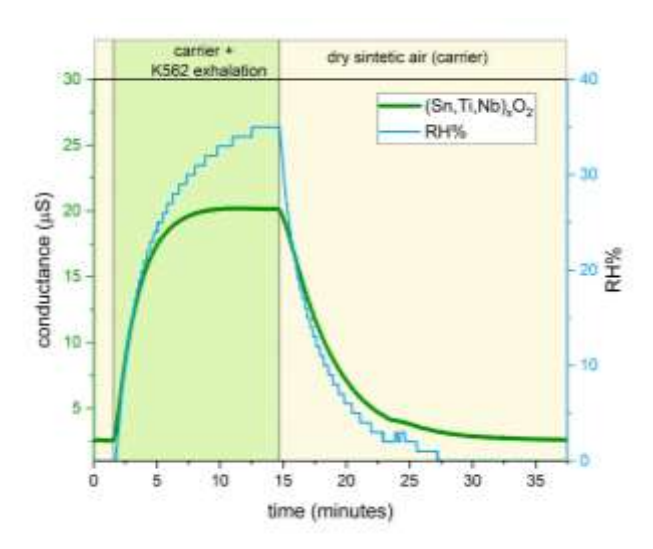
K562 viability assessment. Before conducting the study, and to validate the experimental conditions, the viability of the cell population was monitored over a 6-h period, corresponding to the maximum duration of the experiments. Measurements, performed at regular intervals (0, 2, 4, and 6 h) using the Muse™ Annexin V & Dead Cell Assay (Luminex, USA), confirmed the high robustness of the K562 cell line under the adopted conditions. As demonstrated by the data (Figure 2), cell viability remained consistently above 98% throughout the observation period, with a total apoptotic fraction below 2%. These results confirm that the culture protocol, including the presence of the HEPES buffer, ensures a stable and healthy physiological state for the cells.



**Figure 2.** Flow cytometry dot plots from the Muse<sup>TM</sup> Annexin V & Dead Cell Assay at different time points: t = 0 h, t = 2 h, t = 4 h, and t = 6 h. The plots are divided into four quadrants: live cells (lower-left), early apoptotic (lower-right), late apoptotic/dead (upper-right), and dead (upper-left).

Sensing results. The variation of conductance observed in a chemoresistive gas sensor upon exposure to a gas mixture provides preliminary information regarding the

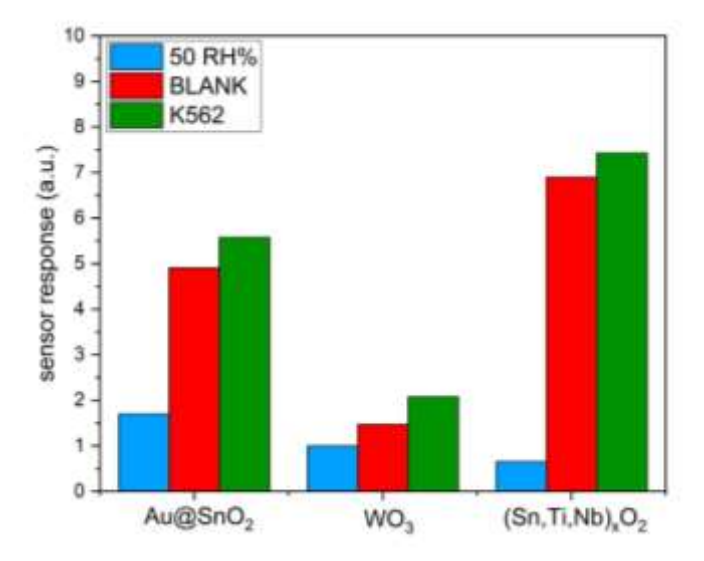
composition of such mixture. Indeed, a sensing layer composed of an n-type semiconducting material exhibits an increase in conductance in the presence of reducing gases, whereas its conductance decreases upon exposure to oxidizing gases. The opposite occurs using a p-type semiconductor as a functional layer. When Au@SnO<sub>2</sub>, WO<sub>3</sub> and (Sn,Ti,Nb)xO<sub>2</sub> were directly exposed to K562 exhalation, a distinct increase in conductance was observed across all tested sensors. Since all materials were n-type, the experiment demonstrated that the gas mixture was mainly composed of reducing gas. Figure 3 illustrates the conductance variation of the (Sn,Ti,Nb)xO<sub>2</sub> sensor, chosen as a representative example of the behavior observed for all devices tested. Following the increase in conductance, the sensors stabilized in a new steady state, indicating that the sensing films were able to find a new equilibrium condition, which did not appear to be perturbed by fluctuations in the composition of the gaseous sample. After returning to the initial conditions of pure dry air, the conductance returned to its baseline value, indicating that the gas sensing process was reversible.



**Figure 3.** (Sn,Ti,Nb)<sub>x</sub>O<sub>2</sub> sensor conductance variation without embedding the pre-concentrator, measured during exposure to K562 exhalation with 50 sccm dry air injection at a temperature of 30 °C.

Figure 3 also displays the growth of RH over time, rising up to 35%. Since usually chemoresistive sensors are highly influenced by moisture, the devices were also exposed to synthetic wet air with a 50 RH%.

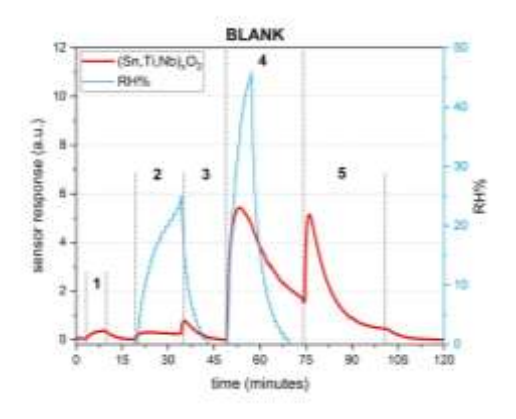
Figure 4 shows the response value of the three sensors to humidity, BLANK and K562, calculated according to Equation (2). These initial measurements were performed without the pre-concentrator to directly assess the intrinsic response of the sensors to the gaseous samples. The Au@SnO2 and (Sn,Ti,Nb)xO2 sensors exhibited a strong response to both the K562 and the BLANK, whereas the WO3 sensor showed a significantly lower response. Finally, the (Sn,Ti,Nb)xO2 sensor demonstrated the lowest sensitivity to humidity among the three materials. Given the high moisture content of the biological samples, this sensor was selected for further investigation to minimize the influence of humidity on subsequent measurements.

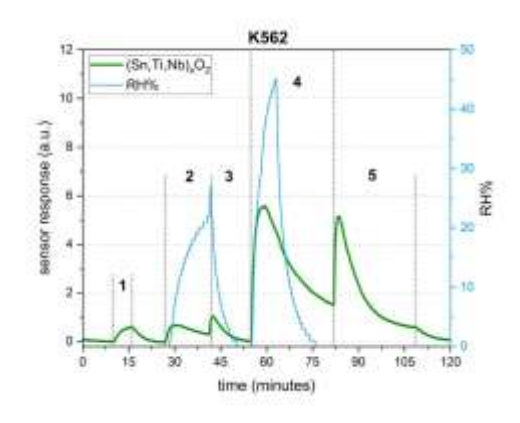


**Figure 4.** Response of the sensors at a temperature of 30 °C vs. wet air (50 RH%; blue bars), and vs. BLANK (green bars) and K562 (red bars).

Notably, for all tested devices, no significant difference was observed between the response to the K562 and to the BLANK. This suggests that the VOCs emitted specifically by the cells were not clearly distinguishable from the background emissions of the culture medium. To address this limitation, a pre-concentrator was integrated into the system. The primary goal was to amplify the signal from cell-emitted VOCs, thereby enhancing the ability to discriminate between the K562 cell signature and that of the culture medium.

Firstly, Cycle 1, using (Sn,Ti,Nb)xO2 as sensor, was applied twice to the system: once with a Petri dish containing only the BLANK, and once with a Petri dish containing the K562 (both positioned in the Chamber-BIO). As shown in Figure 5, which compares the responses for the BLANK and the K562, the overall sensor signals were nearly identical, leading to the conclusion that this method did not provide an advantage in sample targeting compared to the system without a pre-concentrator. However, the use of the pre-concentrator enabled the identification of two distinct desorption peaks, at both 50 °C and 150 °C. This suggests the presence of VOCs with different volatilities, potentially enabling a more refined differentiation of the biological secretion. In this perspective, the characteristics of Carbosieve S-III were ideal for trapping VOCs with very different analyte sizes (C2-C12). Indeed, in Phase 2 (accumulation) the sensor response was very low, mainly due to moisture not retained by the sorbent, while VOCs were only desorbed after heating the pre-concentrator in Phase 4 and 5.





(a) (b)

**Figure 5.** Response of the sensor (Sn,Ti,Nb)<sub>x</sub>O<sub>2</sub> at a temperature of 30 °C with the use of the preconcentrator for (a) BLANK; (b) K562. The measurement procedure consists of multiple sequential phases: **1.** Reference—Desorption at 150 °C for 5 min; **2.** Accumulation—pre-concentrator exposed for 15 min to petri exhalation; **3.** Recovery of sensors baseline in dry air; **4.** First desorption—pre-concentrator heated at 50 °C for 30 min; **5.** Second Desorption—pre-concentrator heated at 150 °C for 30 min.

To improve the discrimination between the response originating from the K562 and the signal from the BLANK, Cycle2 was applied. It should be noted that a pre-test cleaning cycle of the pre-concentrator was performed before each measurement, although it is not shown in the graph. Figure 6 evidenced that a continuous temperature ramp led to a more pronounced difference between the two samples, namely, the signal resulting from the K562 sample exhalation exhibited a greater amplitude. The enhanced targeting performance of this protocol may be attributed to a gas chromatographic-like behavior, made possible by scanning the entire temperature range from 30 °C to 150 °C. In contrast, the desorption approach used in Cycle1, limited to two steps of 50 °C and 150 °C, promoted the release of all lighter VOCs in the initial step, and all heavier ones in the second, without allowing for selective desorption of individual compounds at their optimal temperature.

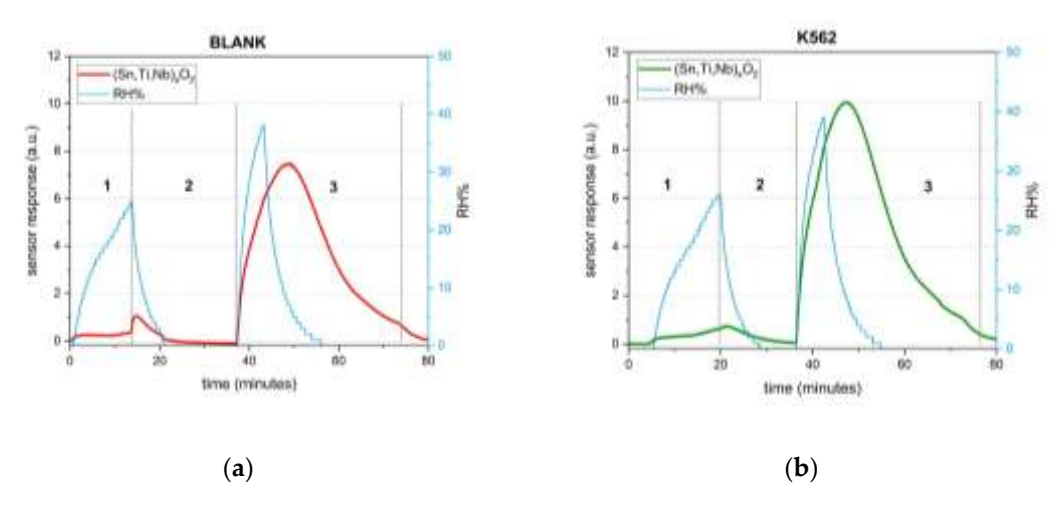


**Figure 6.** Response of the sensor (Sn,Ti,Nb)<sub>x</sub>O<sub>2</sub> in the ramp test with the pre-concentrator at a temperature of 30 °C for (a) BLANK; (b) K562. The measurement procedure consists of multiple sequential phases: **1.** Accumulation—pre-concentrator exposed for 15 min to petri exhalation; **2.** Recovery of sensors baseline in dry air; **3.** Desorption—pre-concentrator heated from 30 °C to 150 °C over 30 min, followed by a 10-min hold at 150 °C.

#### 4. Conclusions

This study offers foundational guidelines for the analysis of cellular exhalation using sensors integrated with a MEMS-based pre-concentrator, which enables pretreatment of gas mixtures. The results of sensing experiments demonstrated the system's potential while also highlighting the inherent challenges of examining cell breathprints. The selection of appropriate sensing material in chemoresistive gas sensors is crucial to mitigate the effects of relative humidity variations on measurements while ensuring high sensitivity to various classes of VOCs. Between several MOXs, (Sn,Ti,Nb)xO2 has been identified as the best candidate for analyzing compounds generated by K562 cell cultures because of its low response to moisture and high reactivity vs. VOCs. However, its inability to discriminate between the culture medium with and without K562 underlines the importance of coupling a gas pretreatment system. The experiments exploiting two cycles

with different temperature-desorption programs explored the capabilities of a pre-concentrator packed with Carbosieve to support the targeting of the biological sample and to provide additional information on the gas composition nature of exhalations (according to gas volatility). Currently, adopting a continuous temperature ramp to desorb preconcentrated VOCs appears to be more promising than a step procedure with a limited number of temperatures. Indeed, Cycle2 led to a more specific targeting of the two samples, namely BLANK and K562. Nonetheless, the results of this work do not exclude that setting temperature desorption steps may not be a practicable strategy. Cycle 1 could be optimized in future, by increasing the number of steps and adjusting their temperatures.

Therefore, future research will focus on fine-tuning the thermal desorption profile (e.g., ramp rate and final temperatures) and on analyzing the profiles using multivariate data analysis techniques (e.g., PCA), with the aim of identifying specific peaks or patterns uniquely attributable to the K562 cell metabolism. Such an approach could lead to the development of a non-invasive and rapid method for monitoring cellular state. The system will also be applied to the study of additional cell cultures in order to validate the approach on a broader scale.

**Author Contributions:** Conceptualization, M.T. and E.S.; methodology, M.T., E.S., S.Z. and G.S.; software, S.Z., L.M. and M.A.; validation, M.T., E.S., E.T. and A.R.; formal analysis, M.T., E.S., M.T.A. and G.B.; investigation, M.T., E.S. and I.E.; resources, B.B., M.B. and G.S.; data curation, M.T. and E.S.; writing—original draft preparation, M.T. and E.S.; writing—review and editing, M.T., E.S., B.B., G.S. and A.R.; visualization, M.T. and E.S.; supervision, B.B. and V.G.; funding acquisition, E.S. All authors have read and agreed to the published version of the manuscript.

**Funding:** This research was supported by the University of Ferrara through the project "BANDO 5x1000 2024", project title: "Study of low-emission systems: design and development of a multifunctional measuring device".

Institutional Review Board Statement: Not applicable.

**Informed Consent Statement:** Not applicable.

**Data Availability Statement:** 

**Conflicts of Interest:** The authors declare no conflict of interest. The funders had no role in the design of the study; in the collection, analyses, or interpretation of data; in the writing of the manuscript; or in the decision to publish the results.

## **Abbreviations**

The following abbreviations are used in this manuscript:

VOCs Volatile Organic Compounds

MOXs Metal-Oxides

MEMS Micro-Electro-Mechanical Systems

RH Relative humidity

# References

- 1. Vander Heiden, M.G.; Cantley, L.C.; Thompson, C.B. Understanding the Warburg Effect: The Metabolic Requirements of Cell Proliferation. *Science* **2009**, 324, 1029–1033. https://doi.org/10.1126/science.1160809.
- 2. Ahmed, D.; Spagnoli, E.; Chakir, A.; Mancinelli, M.; Ferroni, M.; Mehdaoui, B.; El Bouari, A.; Fabbri, B. PrFeTiO<sub>5</sub>-Based Chemoresistive Gas Sensors for VOCs Detection. *Chemosensors* **2025**, *13*, 222. https://doi.org/10.3390/chemosensors13070222.
- 3. Pecunia, V.; Petti, L.; Andrews, J.B.; Ollearo, R.; Gelinck, G.H.; Nasrollahi, B.; Jailani, J.M.; Li, N.; Kim, J.H.; Ng, T.N.; et al. Roadmap on printable electronic materials for next-generation sensors. *Nano Futur.* **2024**, *8*, 032001. https://doi.org/10.1088/2399-1984/ad36ff.

- 4. Guidi, V.; Carotta, M.C.; Fabbri, B.; Gherardi, S.; Giberti, A.; Malagù, C. Array of sensors for detection of gaseous malodors in organic decomposition products. *Sens. Actuators B Chem.* **2012**, *174*, 349–354. [https://doi.org/10.1016/j.snb.2012.07.013.
- 5. Fabbri, B.; Valt, M.; Parretta, C.; Gherardi, S.; Gaiardo, A.; Malagù, C.; Mantovani, F.; Strati, V.; Guidi, V. Correlation of gaseous emissions to water stress in tomato and maize crops: From field to laboratory and back. *Sens. Actuators B Chem.* **2020**, *303*, 127227. https://doi.org/10.1016/j.snb.2019.127227.
- Landini, N.; Anania, G.; Astolfi, M.; Fabbri, B.; Guidi, V.; Rispoli, G.; Valt, M.; Zonta, G.; Malagù, C. Nanostructured Chemoresistive Sensors for Oncological Screening and Tumor Markers Tracking: Single Sensor Approach Applications on Human Blood and Cell Samples. Sensors 2020, 20, 1411. https://doi.org/10.3390/s20051411.
- 7. Astolfi, M.; Rispoli, G.; Benedusi, M.; Zonta, G.; Landini, N.; Valacchi, G.; Malagù, C. Chemoresistive Sensors for Cellular Type Discrimination Based on Their Exhalations. *Nanomaterials* **2022**, *12*, 1111. https://doi.org/10.3390/nano12071111.
- 8. Roy Morrison, S. *The Chemical Physics of Surfaces*, 1st ed.; Springer: New York, NY, USA, 2012; https://doi.org/10.1007/978-1-4615-8007-2.
- Spagnoli, E.; Valt, M.; Gaiardo, A.; Fabbri, B.; Guidi, V. Insights into the Sensing Mechanism of a Metal-Oxide Solid Solution via Operando Diffuse Reflectance Infrared Fourier Transform Spectroscopy. Nanomaterials 2023, 13, 2708. https://doi.org/10.3390/nano13192708.
- Ortega, P.P.; Gherardi, S.; Spagnoli, E.; Fabbri, B.; Landini, N.; Malagù, C.; Macchi, C.; Aldao, C.M.; Ponce, M.A.; Simões, A.Z.; et al. Deciphering the CO sensing mechanisms of CeO<sub>2</sub>-based nanostructured semiconductors: Influence of doping, morphology, and humidity. Sens. Actuators B Chem. 2025, 440, 137921. https://doi.org/10.1016/j.snb.2025.137921.
- 11. Degler, D.; Junker, B.; Allmendinger, F.; Weimar, U.; Barsan, N. Investigations on the temperature-dependent interaction of water vapor with tin dioxide and its implications on gas sensing. *ACS Sens.* **2020**, *5*, 3207–3216. https://doi.org/10.1021/acssensors.0c01493.
- 12. Madou, M.J.; Morrison, S.R. Chemical Sensing with Solid State Devices; Elsevier: Amsterdam, The Netherlands, 1989. https://doi.org/10.1016/C2009-0-22258-6.
- 13. Zampolli, S.; Elmi, I.; Mancarella, F.; Betti, P.; Dalcanale, E.; Cardinali, G.C.; Severi, M. Real-time monitoring of sub-ppb concentrations of aromatic volatiles with a MEMS-enabled miniaturized gas-chromatograph. *Sens. Actuators B Chem.* **2009**, *14*, 322–328. https://doi.org/10.1016/j.snb.2009.06.021.
- 14. Zampolli, S.; Elmi, I.; Cardinali, G.C.; Masini, L.; Bonafè, F.; Zardi, F. Compact-GC platform: A flexible system integration strategy for a completely microsystems-based gas-chromatograph. *Sens. Actuators B Chem.* **2020**, 305, 127444. https://doi.org/10.1016/j.snb.2019.127444.
- 15. Lozzio, C.B.; Lozzio, B.B. Human chronic myelogenous leukemia cell-line with positive Philadelphia chromosome. *Blood* **1975**, 45, 321–334. https://doi.org/10.1182/blood-2016-08-736025.
- 16. Capuano, R.; Talarico, R.V.; Spitalieri, P.; Roberto, P.; Giuseppe, N.; Sangiuolo, F.; Di Natale, C. GC/MS-based Analysis of Volatile Metabolic Profile Along in vitro Differentiation of Human Induced Pluripotent Stem Cells. *Bio-protocol* **2017**, 7, e2642. https://doi.org/10.21769/BioProtoc.2642.
- 17. Spagnoli, E.; Fabbri, B.; Gaiardo, A.; Valt, M.; Ardit, M.; Krik, S.; Cruciani, G.; Della Ciana, M.; Vanzetti, L.; Vola, G.; et al. Design of a metal-oxide solid solution for selective detection of ethanol with marginal influence by humidity. *Sens. Actuators B Chem.* **2022**, *370*, 132426. https://doi.org/10.1016/j.snb.2022.132426.
- 18. Spagnoli, E.; Krik, S.; Fabbri, B.; Valt, M.; Ardit, M.; Gaiardo, A.; Vanzetti, L.; Della Ciana, M.; Cristino, V.; Vola, G.; et al. Development and characterization of WO<sub>3</sub> nanoflakes for selective ethanol sensing. *Sens. Actuators B Chem.* **2021**, 347, 130593. https://doi.org/10.1016/j.snb.2021.130593.
- 19. Rossi, A.; Spagnoli, E.; Tralli, F.; Marzocchi, M.; Guidi, V.; Fabbri, B. New Approach for the Detection of Sub-ppm Limonene:
  An Investigation through Chemoresistive Metal-Oxide Semiconductors. *Sensors* **2023**, 23, 6291. https://doi.org/10.3390/s23146291.
- 20. Astolfi, M.; Zonta, G.; Gherardi, S.; Malagù, C.; Vincenzi, D.; Rispoli, G. A Portable Device for I–V and Arrhenius Plots to Characterize Chemoresistive Gas Sensors: Test on SnO<sub>2</sub>-Based Sensors. *Nanomaterials* **2023**, 13, 2549. https://doi.org/10.3390/nano13182549.
- 21. Spagnoli, E.; Gaiardo, A.; Fabbri, B.; Valt, M.; Krik, S.; Ardit, M.; Cruciani, G.; Della Ciana, M.; Vanzetti, L.; Vola, G.; et al. Design of a Metal-Oxide Solid Solution for Sub-ppm H<sub>2</sub> Detection. *ACS Sens.* **2022**, 7, 573–583. https://doi.org/10.1021/acssensors.1c02481.

Disclaimer/Publisher's Note: The statements, opinions and data contained in all publications are solely those of the individual author(s) and contributor(s) and not of MDPI and/or the editor(s). MDPI and/or the editor(s) disclaim responsibility for any injury to people or property resulting from any ideas, methods, instructions or products referred to in the content.